Modeling of Bedrock Groundwater Levels Based on Antecedent Precipitation Indices

Ken'ichirou KOSUGI[1,2,*], Masamitsu FUJIMOTO[3], Yosuke YAMAKAWA[4], Naoya MASAOKA[1], Tetsushi ITOKAZU[1] and Takahisa MIZUYAMA[1]

[1] Graduate School of Agric., Kyoto University (Kitashirakawa, Sakyo-ku, Kyoto, Kyoto 6068502, Japan)
[2] JST, CREST (Sanbancho, Chiyoda-ku, Tokyo 1020075, Japan)
[3] College of Science and Engineering, Ritsumeikan University (Nojihigasi, Kusatsu, Shiga 5288577, Japan)
[4] Agric. and Forestry Research Center, University of Tsukuba (Ikawa, Aoi-ku, Shizuoka, 4280504, Japan)
*Corresponding author. E-mail: kos@kais.kyoto-u.ac.jp

Bedrock groundwater is reported to be one of the main factors governing the occurrence of deep-seated landslides. Hence, predictions of changes in bedrock groundwater level (BGL) caused by rainwater infiltration are essential for assessments of landslide vulnerability as well as for establishment of effective evacuation systems. This study evaluates four simple functional models that correlate antecedent precipitation indices (APIs) with BGL. The results showed that the models exhibit great applicability to BGL observed at 25 boreholes excavated at five different locations. By using an appropriate model chosen for each borehole, we evaluated BGL conditions at the initiation of the Niigata and Tohoku earthquakes. The results revealed that the Niigata earthquake occurred at a higher BGL than the Tohoku earthquake did, which explained the differences in the number and magnitude of deep-seated landslides associated with these earthquakes.

Key words: deep-seated landslide, bedrock groundwater, antecedent precipitation index

1. INTRODUCTION

Bedrock groundwater is reported to be one of the main factors governing the occurrence of deep-seated landslides. Under a heavy storm event, an increase in bedrock groundwater level (BGL) beyond a critical value can be a direct cause of a deep-seated landslide [*Jitousono et al.*, 2004]. The BGL at the initiation of an earthquake may play a role in controlling the number and magnitude of deep-seated landslides triggered by the earthquake [*Chigira et al.*, 2012; *Tsutsumi and Fujita*, 2012]. Hence, predictions of changes in BGL caused by rainwater infiltration are essential for assessment of landslide vulnerability as well as for establishment of effective evacuation systems.

This study evaluates a method to estimate BGL using antecedent precipitation indices (APIs), which are frequently used to evaluate the residual effects of previous precipitation on soil moisture [e.g., *Sittner et al.*, 1969] or storm runoff [e.g., *Fedora and Beschta*, 1989]. In this study, we examine the applicability of four simple functional models that correlate APIs with the BGL observed at 25 boreholes. Using an appropriate model for each borehole, we discuss the BGLs at the initiation of two major earthquakes in Japan.

2. METHOD

2.1 Functional models

The antecedent precipitation index (API) X [mm] with a half-life time (HLT) M [h] can be calculated as

$$X(t) = X(t-1)e^{\alpha} + R(t)e^{\alpha/2} \quad (1)$$

where $X(t)$ and $X(t - 1)$ represent API at times t [h] and t - 1 [h], respectively, and $R(t)$ [mm] is the rainfall amount between t - 1 and t [*Suzuki and Kobashi*, 1981; *Descroix et al.*, 2002]. The reduction coefficient α [h^{-1}] is related to M by

$$\alpha = \ln(0.5)/M \quad (2)$$

This study evaluates the following four simple functional models that correlate APIs with BGL [*Kosugi et al.*, 2013]

$$H = b_0 + b_1 X_1 \quad (3)$$

$$H = b_0 + b_1 X_1 + b_2 X_2 \quad (4)$$

$$H = b_0 + b_1 X_1^{p_1} \quad (5)$$

$$H = b_0 + b_1 X_1^{p_1} + b_2 X_2^{p_2} \quad (6)$$

where H is BGL observed from the ground surface, X_1 is an API with a long HLT (M_1), X_2 is an API with a short HLT (M_2), and b_0, b_1, b_2, p_1, and p_2 are parameters to be optimized. The Li1 (Eq. (3)) and the Li2 models (Eq. (4)) assume linear relationships between BGL and APIs, and the Pw1 (Eq. (5)) and Pw2 models (Eq. (6)) employ power functions. Whereas the Li1 and Pw1 models use an API with a single HLT, the Li2 and Pw2 models use two APIs with two different HLTs.

2.2 BGL observation sites

The performance of the four models was examined using annual hydrographs of BGL observed at 25 boreholes from the five locations shown in **Fig. 1**.

Mt. Rokko in Hyogo Prefecture is underlain by weathered granitic bedrock. In the Mt. Rokko ridge (**Fig. 1a**; 34°46'N, 135°16'E), eight boreholes were excavated on a steep hillside slope of average inclination 40°. In the Mt. Rokko foothill region (**Fig. 1b**; 34°40–42'N, 135°7–10'E), three boreholes were excavated around the outlets of forested catchments. The average values of annual precipitation are 1,600 and 1,200 mm for the ridge and foothill regions, respectively. The depth and average water table height of each borehole are summarized in **Table 1**.

Yotagiri watershed, shown in **Fig. 1c** (35°41'N, 137°51'E), is situated in the Kiso mountain range in Nagano Prefecture. The watershed is underlain by granodioritic bedrock and has an average annual precipitation of 2,500 mm. The BGLs observed at five boreholes were analyzed.

Asatani watershed, shown in **Fig. 1d** (33°49'N, 133°28'E), is located in the upstream region of the Yoshino River in Kochi Prefecture and is underlain by schistous bedrock. The average annual precipitation of the watershed is 2,600 mm. The BGLs observed at five boreholes were analyzed. Boreholes A1 through A4 were located in the central area of the catchments, and Borehole A5 was situated around the outlet of the catchments.

In Harihara watershed, a deep-seated landslide was triggered by a heavy storm event that took place in July 1997 (**Fig. 1e**; 32°8'N, 130°22'E). Our study analyzed the BGLs observed at four boreholes excavated around the landslide scar. The shallow part of the bedrock consists of andesite underlain by tuff. The groundwater that was monitored had

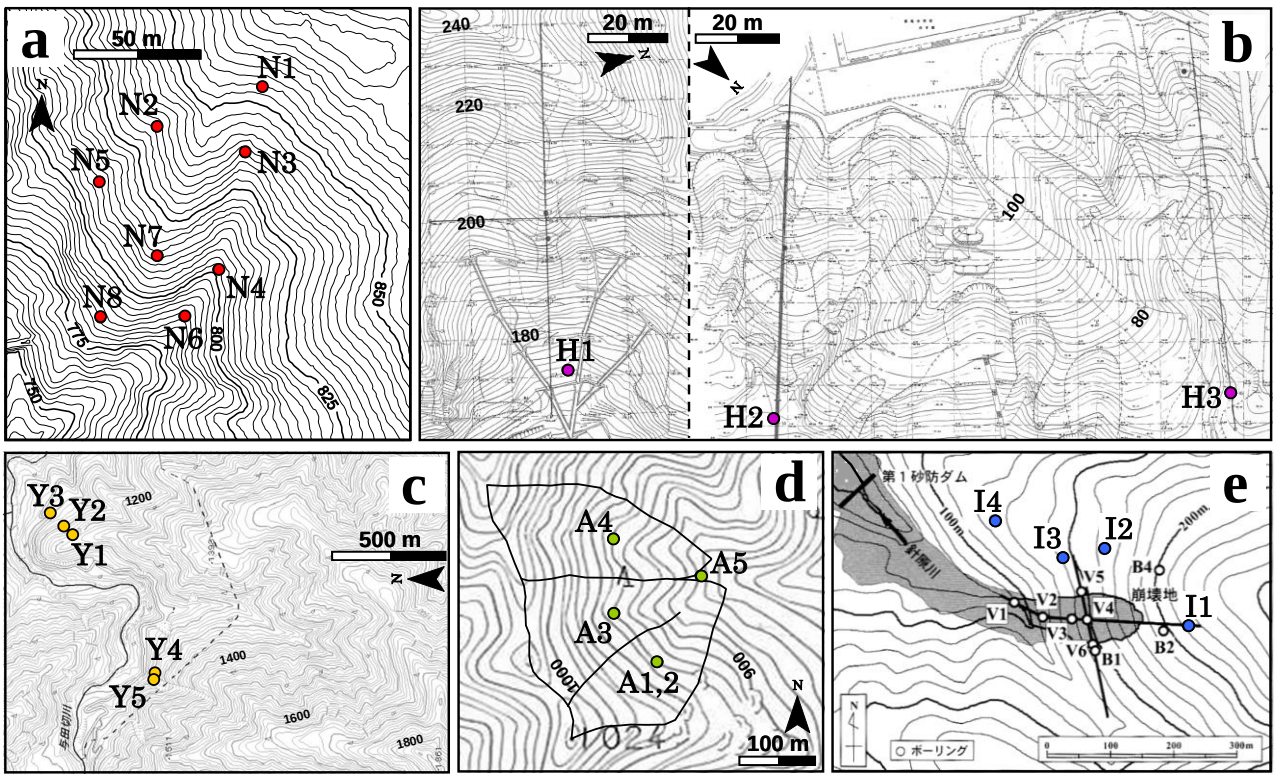

Fig. 1 Topography and borehole locations for (a) Rokko ridge, (b) Rokko foothill, (c) Yotagiri, (d) Asatani, and (e) Harihara regions

formed in the andesitic bedrock. The watershed's average annual precipitation is 2,300 mm.

Detailed information of the observation sites is presented in *Kosugi et al.* [2014].

2.3 Model applications

The four functional models were applied to reproduce an annual BGL hydrograph observed at 1-hour intervals at each of the 25 boreholes. The parameters were optimized to maximize the Nash–Sutcliffe efficiency factor (NSEF):

$$\mathrm{NSEF} = 1 - \sum_i \left(H_{obs,i} - H_{cal,i}\right)^2 \Big/ \sum_i \left(H_{obs,i} - \overline{H}_{obs}\right)^2 \tag{7}$$

where H_{obs} and H_{cal} represent the observed and computed BGL, respectively, and $\overline{H}_{obs}$ is the average BGL height. Selection of the most appropriate model was made using Akaike's information criterion [*Akaike*, 1973], which considers both the residual errors and the number of parameters of the model. To eliminate the effects of the initial conditions, preliminary API calculations were conducted for a period of around 2 years before the time of our modeling study [*Kosugi et al.*, 2014].

2.4 Estimation of BGL preceding earthquakes

The BGL at the initiation of an earthquake is reportedly one of the primary factors controlling the number and magnitude of deep-seated landslides triggered by the earthquake.

When "the mid Niigata prefecture earthquake in 2004 (the Niigata earthquake)" occurred on October 23, 2004, the recorded acceleration in Nagaoka City, Niigata Prefecture, was 920.9 gal. Around Nagaoka City, 3,791 landslides were caused by the earthquake, including 362 deep-seated landslides [*Niigata Prefecture Civil Engineering Division*, 2005]. Three days before the earthquake, Nagaoka City experienced a rainstorm with a total precipitation of 119 mm, and it is reported that the wet initial conditions caused by this storm event contributed to an increase in the number and magnitude of deep-seated landslides [*Chigira et al.*, 2012].

In contrast, there was no accompanying major storm before "the 2011 off the Pacific coast of Tohoku earthquake (the Tohoku earthquake)" on March 11, 2011. Although an acceleration of 1807.8 gal was recorded in Sendai City, Miyagi Prefecture, the number and magnitude of landslides associated with this earthquake were significantly less than those caused by the Niigata earthquake [*Tsutsumi and Fujita*, 2012]. This is presumably due to the relatively dry conditions before the earthquake.

For the purpose of conducting quantitative comparisons of the slope wetness conditions between the Niigata and the Tohoku earthquakes, we examined the BGLs estimated by the above functional models, *i.e.,* the BGLs over a period of 3 years prior to the earthquakes were computed using the model determined as most appropriate for each of the 25 boreholes. Then, the BGLs at the initiation of the earthquakes were compared with the BGLs for the period of 3 years prior to the earthquakes to elucidate the wetness conditions immediately prior to the earthquakes. For these analyses, we used hourly precipitation data observed by the Japan Meteorological Agency at Nagaoka station from the Automated Meteorological Data Acquisition System (37°27.0'N, 138°49.4'E; 23.0 m a.s.l.) and at Sendai observatory (38°15.7'N, 140°53.8'E; 38.9 m a.s.l.). The calculations of BGL were started 5 years before the earthquakes took place to eliminate the effects of differences in the initial API values.

3. RESULTS AND DISCUSSION

3.1 Model application

3.1.1 BGL observed at Borehole I3

Figure 2 summarizes the model results obtained for Borehole I3 in Harihara watershed (**Fig. 1e**). In **Fig. 2a**, along with the annual hyetograph, the APIs with HLTs of 72 and 1.5 h are shown. In Japan, a combination of the APIs with HLTs of 72 and 1.5 h have been widely used for providing accurate information to evaluate vulnerabilities for shallow landslide and debris flow occurrences. Here, the API with HLT of 72 is used as an index to evaluate the cumulative effects of precipitation, whereas the API with HLT of 1.5 is used as an index to evaluate the effects of rainfall intensity.

When the APIs with HLT values of 72 and 1.5 h were used for X_1 and X_2 in the Li2 model (i.e., Eq. (4)) and b_0, b_1, b_2 were optimized, the resulting H values were as shown in **Fig. 2c**. The model produced several contradictions with the observed BGL hydrograph, *i.e.,* the computed H exhibited more peaky responses than the observed H and could not reproduce the seasonal variations in the observed hydrograph. **Figure 2d** compares X_1 and X_2 values obtained for each time point. The color of each plot represents the range of the observed H value. Correlations among the abscissa, ordinate, and the color of each plot are indistinct, indicating that the combination of the X_1 and X_2 cannot distinguish the observed BGL.

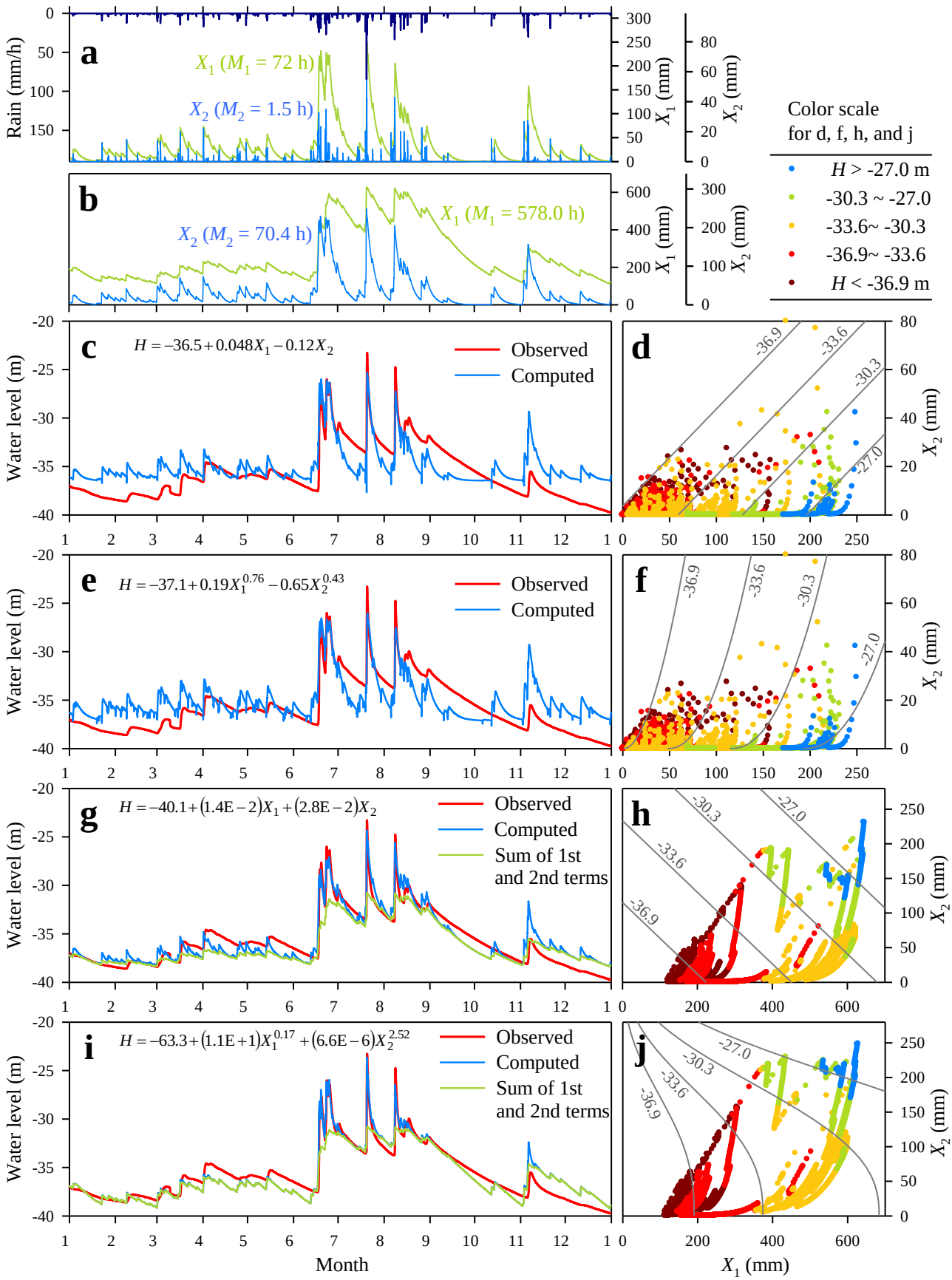

Fig. 2 (a, b) Hourly rainfall and APIs, (c, e, g, i) observed and computed BGLs, and (d, f, h, j) Snake-line plots for the borehole I3

Table 1 Properties and optimized parameters of each borehole

Point	BD[1)] (m)	AWH[2)] (m)	Model	NSEF	M_1 (h)	M_2 (h)	p_1	p_2	b_0 (m)	b_1 m/mm^{p1}	b_2 m/mm^{p2}
N1	69	-57.5	Pw2	0.832	479.0	71.4	0.60	5.46	-74.1	7.93E-01	1.98E-12
N2	65	-47.3	Pw1	0.962	769.8	-	0.72	-	-60.0	2.27E-01	-
N3	70	-50.7	Pw1	0.914	1114.4	-	1.09	-	-62.0	1.59E-02	-
N4	38	-18.3	Li1	0.916	1138.7	-	1.00	-	-29.4	2.67E-02	-
N5	45	-35.7	Pw2	0.970	854.3	89.2	0.99	8.22	-42.3	2.20E-02	6.22E-19
N6	21	-13.4	Pw2	0.968	904.1	44.6	1.52	3.70	-16.2	3.82E-04	1.41E-08
N7	52	-44.1	Pw2	0.976	1117.6	68.6	1.23	3.43	-46.7	1.55E-03	5.64E-08
N8	25	-13.8	Pw2	0.974	1061.3	76.8	0.75	3.16	-16.1	2.68E-02	1.20E-07
H1	20	-8.6	Pw1	0.596	462.6	-	0.06	-	-120.7	8.54E+01	-
H2	20	-5.6	Pw2	0.843	1398.2	182.2	0.05	2.39	-18.7	9.66E+00	1.28E-05
H3	6	-4.1	Pw2	0.903	434.3	82.8	0.05	1.00	-13.3	7.03E+00	1.31E-02
Y1	30	-25.9	Pw1	0.694	17.9	-	0.49	-	-28.8	1.38E+00	-
Y2	30	-24.1	Pw1	0.592	151.3	-	0.55	-	-28.3	3.57E-01	-
Y3	39	-19.9	Pw1	0.842	324.8	-	0.81	-	-27.3	1.02E-01	-
Y4	20	-10.5	Pw1	0.772	77.5	-	0.83	-	-12.0	7.30E-02	-
Y5	25	-7.5	Pw1	0.807	73.8	-	0.81	-	-9.0	8.39E-02	-
A1	17	-5.5	Pw1	0.683	154.7	-	0.69	-	-6.1	3.21E-02	-
A2	45	-3.0	Pw1	0.810	167.6	-	0.58	-	-4.2	9.88E-02	-
A3	45	-5.4	Pw2	0.887	95.3	8.9	0.47	2.24	-5.8	6.58E-02	2.27E-05
A4	45	-3.6	Pw2	0.857	166.6	8.6	0.05	1.08	-5.2	1.25E+00	1.48E-02
A5	30	-2.4	Pw2	0.566	140.7	3.1	0.52	0.73	-4.0	1.65E-01	3.98E-02
I1	40	-18.7	Pw2	0.845	286.9	81.2	0.05	1.06	-56.7	2.97E+01	1.98E-02
I2	87	-44.0	Pw2	0.892	821.4	62.2	0.67	7.21	-54.5	2.05E-01	8.90E-18
I3	65	-35.7	Pw2	0.951	578.0	70.4	0.17	2.52	-63.3	1.05E+01	6.63E-06
I4	80	-30.0	Pw2	0.879	340.6	199.7	0.05	6.68	-128.2	7.71E+01	1.81E-17

1) Borehole depth, 2) Average water table height

Figures 2e and **2f** show results for the Pw2 model when the APIs with HLTs of 72 and 1.5 h were used for X_1 and X_2, respectively, in Eq. (6). Although b_0, b_1, b_2, p_1, and p_2 were optimized, the model produced similar contradictions to **Figs. 2c** and **2d**. Thus, the results in **Fig. 2c** through **2f** clearly indicate that the HLTs of 72 h and 1.5 h, which are widely used for predicting shallow landslides and debris flows, do not represent the groundwater dynamics at Borehole I3.

When the HLTs (i.e., M_1 and M_2) of the Li2 model were optimized, the performance of the model was dramatically improved (**Fig. 2g**), *i.e.*, the plots of Eq. (4) reproduced a peaky response for each storm event as well as gradual seasonal variations of the observed BGL. M_1 and M_2 were optimized at 607.6 and 45.5 h, respectively, both of which were considerably larger than the values used for the shallow landslide and debris flow predictions. In **Fig. 2h**, the color for each plot is clearly correlated with the abscissa and ordinate, indicating that the combination of the optimized X_1 and X_2 can accurately describe the BGL observed at Borehole I3.

The Pw2 model displayed further improvements in the estimations of BGL (**Fig. 2i**) when M_1 and M_2 in Eq. (6) were optimized. The derived M_1 and M_2 were 578.0 and 70.4 h, respectively. The time series of X_1 and X_2 with these HLTs are shown in **Fig. 2b**. Compared with the Li2 model in **Fig. 2g**, the Pw2 model improved estimations of peak values in June and July. Additionally, the peaky responses from January through May and November through December became less remarkable, producing close matches with the observed BGL hydrograph. In **Fig. 2j**, the non-linear theoretical H contours were derived from the Pw2 model, which agreed well with the observed H values. Based on Akaike's information criterion, the Pw2 model performed best among the four models.

3.1.2 Results for the 25 boreholes

Table 1 summarizes the model results for the 25 boreholes. The Pw2 model performed best for 14 of the boreholes, and the Pw1 and Li1 models were shown to perform best for 10 boreholes and one borehole, respectively. In general, we derived accurate estimations of the observed BGLs as indicated by the NSEF values in **Table 1**, which were greater than ~0.8 for many of the boreholes.

Several boreholes in the Mt. Rokko foothill

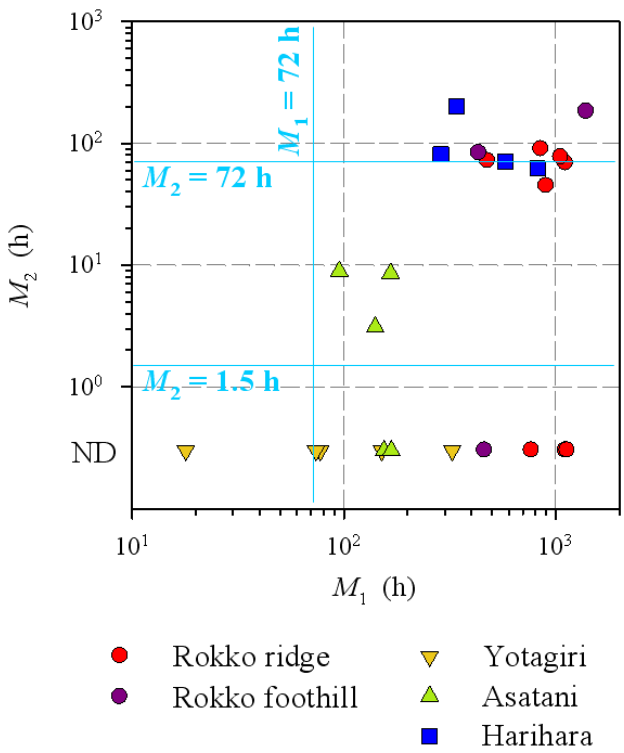

Fig. 3 Relationship between M_1 and M_2 (ND on ordinate axis stands for no-data.)

region, Yotagiri watershed, and Asatani watershed produced relatively small NSEF values, which were nevertheless >5.66.

Optimized HLTs for the 25 boreholes are shown in **Fig. 3**. Whereas M_1 displayed a broad range, 17.9–1398.2 h, its value was greater than the value commonly used for shallow landslide and debris flow predictions (72 h) for most of the boreholes. This indicated that for predicting deep-seated landslides, we should consider the cumulative effects of antecedent precipitation for a longer period than is generally used in the prediction of shallow landslides and debris flows.

The values of M_2 ranged from 3.1 to 199.7 h, greater than the value of 1.5 h commonly used for evaluating the effects of rainfall intensity for shallow landslide and debris flow predictions. For many of the boreholes, M_2 was optimized at around 72 h. The HLT of 72 h has been commonly used for evaluating the cumulative effects of precipitation for shallow landslide and debris flow predictions. Therefore, these M_2 values suggests the possible contribution of bedrock groundwater to the initiation of shallow landslides and debris flows, *i.e.*, the faster responses of bedrock groundwater may contribute additional water supplies to the shallow soil layer, resulting in acceleration of soil mass movements. This outcome coincides well with the results of *Kosugi et al.* [2012], who clarified the roles of bedrock groundwater in the occurrence of shallow landslides.

The values of M_1 and M_2 are generally large for the Mt. Rokko regions underlain by granitic bedrock and Harihara watershed underlain by andesitic bedrock, and relatively small for the Yotagiri watershed underlain by granodioritic bedrock and the Asatani watershed underlain by schistous bedrock. Thus, the variability in HLTs between locations tended to be greater than the variability within a location. This suggests that the geological characteristics for each location had a greater effect on BGL than did the characteristics of each point

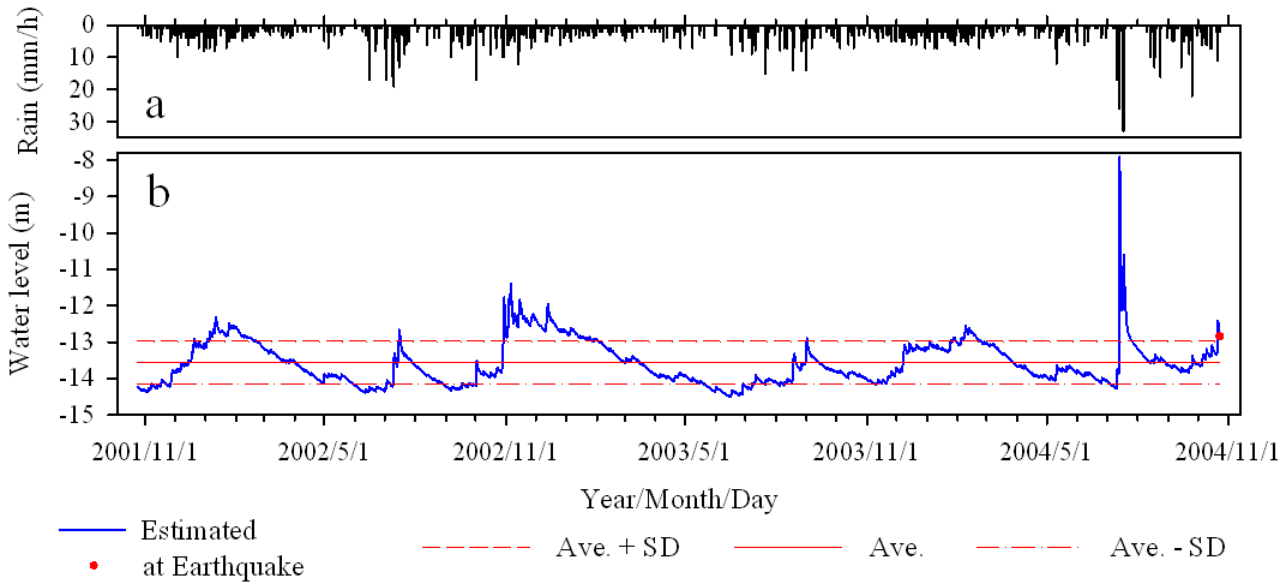

Fig. 4 (a) Hyetograph and (b) BGLs for 3 years before the Niigata earthquake computed by using the Pw2 model with the parameters optimized for the borehole N8

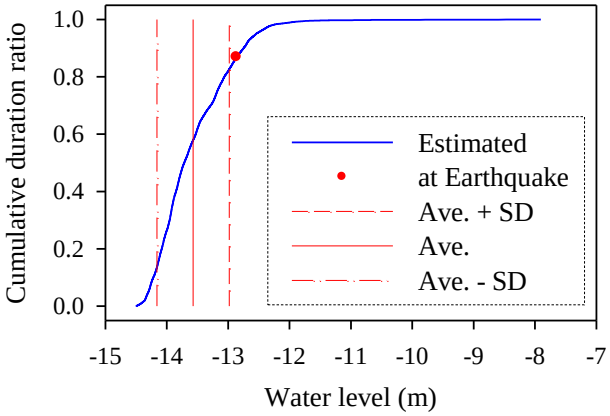

Fig. 5 BGL-duration curve for 3 years before the Niigata earthquake computed by using the Pw2 model with the parameters optimized for the borehole N8

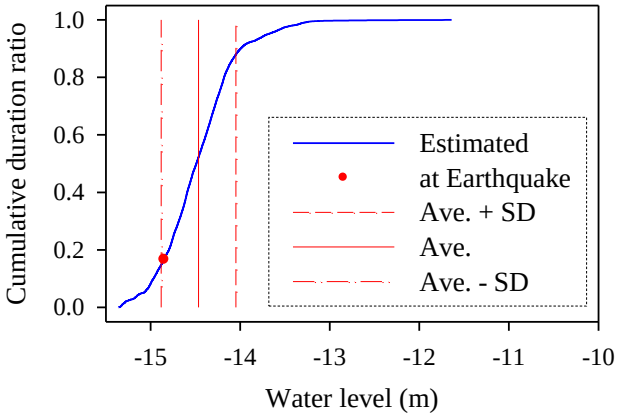

Fig. 7 BGL-duration curve for 3 years before the Tohoku earthquake computed by using the Pw2 model with the parameters optimized for the borehole N8

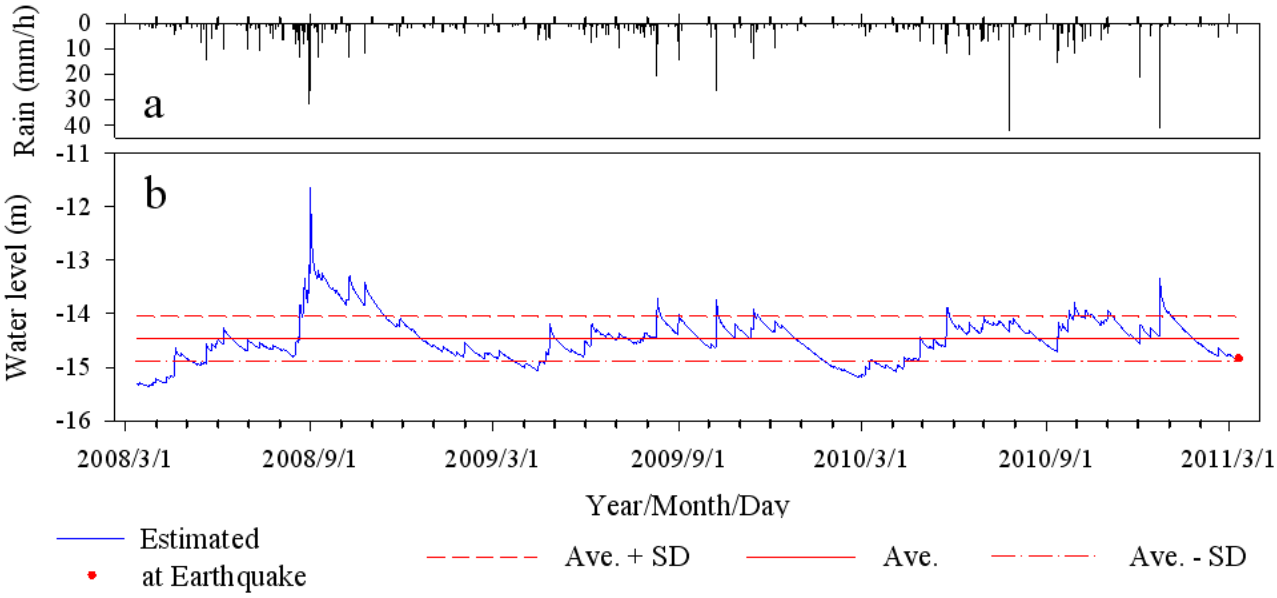

Fig. 6 (a) Hyetograph and (b) BGLs for 3 years before the Tohoku earthquake computed by using the Pw2 model with the parameters optimized for the borehole N8

situated in the same geological setting.

3.2 BGL at the initiation of earthquakes

3.2.1 BGL estimated by the parameters for Borehole N8

Figure 4b shows the BGL computed for a period of 3 years prior to the Niigata earthquake using the Pw2 model with the parameters optimized for Borehole N8 (**Table 1**). The red circle indicates the BGL at the initiation of the earthquake, which was significantly higher than the average BGL over the 3 years. For quantitative evaluation of the water level, we computed the normalized water level H^*, which is defined as:

$$H^* = (H - \mu)/\sigma \,, \tag{8}$$

where H is the BGL at the initiation of the earthquake, and μ and σ are the average and standard deviation, respectively, of the BGL for a period of 3 years before the earthquake. In the case shown in **Fig. 4b**, the computed H^* was large, with a value of 1.20. **Figure 4** indicates that the high BGL at the initiation of the earthquake was attributable not only to the storm event just before the earthquake but also to the heavy storm event in July 2004 and a series of storms from August to October 2004 (**Fig. 4a**).

In **Fig. 5**, a BGL-duration curve has been drawn by rearranging the hydrograph in **Fig. 4b** according

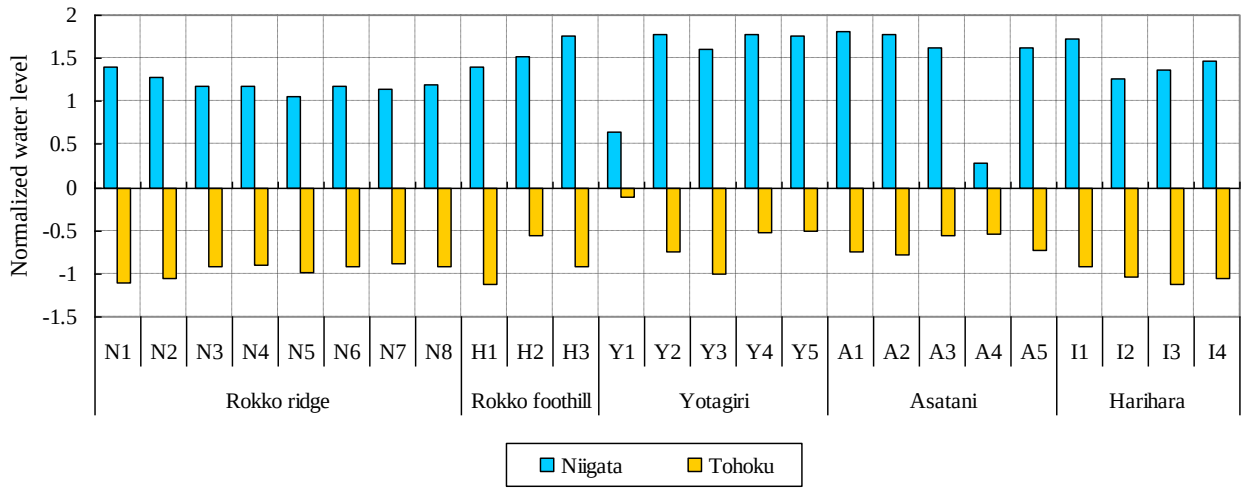

Fig. 8 Normalized water level at initiations of the Niigata and Tohoku earthquakes

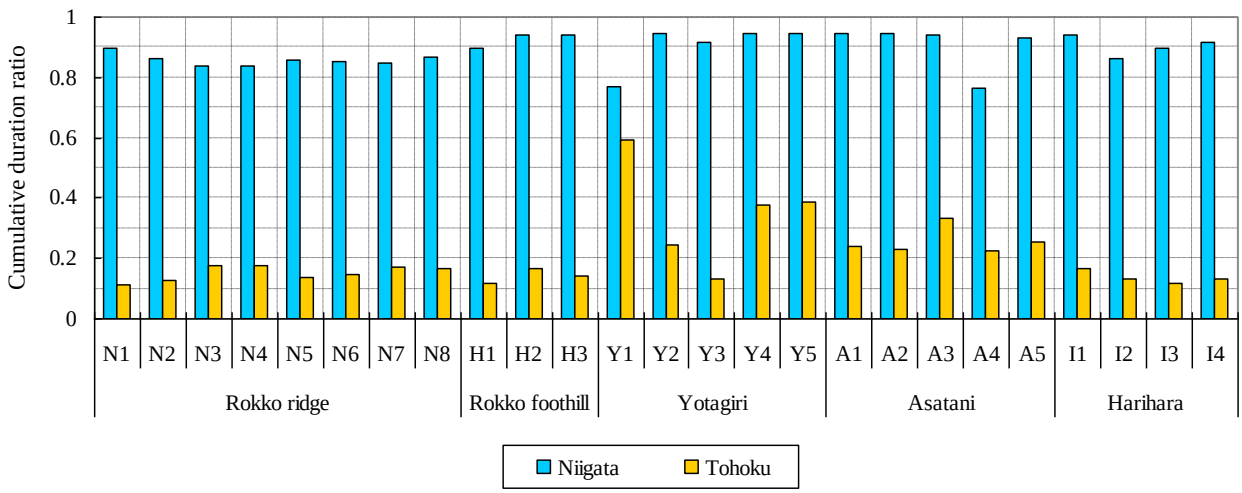

Fig. 9 Cumulative duration ratio of BGL at initiations of the Niigata and Tohoku earthquakes

to the order of the BGL values. The ordinate indicates the cumulative duration ratio in the 3-year period in which the BGL magnitude was equal to or smaller than the BGL given in the abscissa. The red circle corresponds to the initiation of the Niigata earthquake. The cumulative duration ratio at the initiation of the earthquake, which was 0.87 for the case shown in **Fig. 5**, can also be used for evaluating BGL.

Figure 6b shows the BGL computed for a period of 3 years before the Tohoku earthquake using the Pw2 model with the parameters optimized for Borehole N8. In contrast to the case shown in **Fig. 4**, the BGL at the initiation of the earthquake was low because of lower antecedent precipitation (**Fig. 6a**). The computed normalized water level H^* (= -0.92) was considerably smaller than that for the Niigata earthquake. The negative H^* value indicates that the water level at the initiation of the Tohoku earthquake was lower than the average value. The BGL-duration curve shown in **Fig. 7** indicates that the cumulative duration ratio at the initiation of the Tohoku earthquake was 0.17, which was around one fifth that for the Niigata earthquake (**Fig. 5**).

It can be seen from **Figs. 4–7** that the Niigata earthquake occurred under higher BGL than the Tohoku earthquake did for the point representing BGL behaviors similar to those observed at Borehole N8.

3.2.2 BGLs estimated from the parameters for the 25 boreholes

We conducted similar analyses, as shown in **Figs. 4–7**, using the model determined as most appropriate for each of the 25 boreholes (**Table 1**). **Figures 8** and **9** show the normalized water level and cumulative duration ratio, respectively, derived for each borehole and earthquake.

For every borehole, the normalized water level at the initiation of the Niigata earthquake was positive and greater than that at the initiation of the

Tohoku earthquake, which was negative (**Fig. 8**). In **Fig. 9**, the cumulative duration ratios at the initiation of the Niigata earthquake were higher than 0.76 for all boreholes and considerably greater than those at the initiation of the Tohoku earthquake, except for Borehole Y1. For Borehole Y1, the cumulative duration ratio was relative large at the initiation of the Tohoku earthquake, which is attributable to the fact that the M_1 value of this borehole (**Table 1**) is the lowest of all the boreholes. Because of the small M_1 value, the BGLs of Borehole Y1 were significantly affected by an adjacent storm event; *i.e.*, a light storm event with a total precipitation of 8.5 mm, which occurred two days before the Tohoku earthquake (**Fig. 6a**), resulted in the relatively large cumulative duration ratio for Borehole Y1.

From the results shown in **Figs. 8** and **9**, we concluded that the Niigata earthquake occurred under higher BGL conditions than the Tohoku earthquake at the various points, which represent BGL behaviors similar to those observed at the points summarized in **Table 1**.

4. CONCLUSIONS

This study evaluated four simple functional models that correlate antecedent precipitation indices (APIs) with bedrock groundwater levels (BGLs). The Li1 and Li2 models assumed linear relationships between the BGLs and APIs, and the Pw1 and Pw2 models employed power functions. The Li1 and Pw1 models used an API with a single half-life time (HLT), whereas Li2 and the Pw2 models used two APIs with two different HLTs.

The performances of the models were examined using BGLs observed at 25 boreholes excavated at five different locations. The results showed that the Pw2 model performed best for reproducing the BGL observed at 14 of the boreholes. The Pw1 and Li1 models performed best for 10 boreholes and one borehole, respectively. The optimized HLTs, which were significantly longer than the values generally used for predictions of shallow landslides and debris flows, accurately represented groundwater dynamics. In general, the optimized parameters showed typical values for each location, suggesting that the geological characteristics at each location had a greater effect on the changes in BGL than did the characteristics of each point situated in the same geological settings.

Using an appropriate model chosen for each borehole, the BGL conditions at the initiation of two major earthquakes were evaluated. The results confirmed that the Niigata earthquake occurred under conditions of higher BGL relative to the Tohoku earthquake, which partly explained the differences in the number and magnitude of deep-seated landslides associated with these earthquakes.

The functional models can, without difficulty, estimate BGLs during storms, as well as at the initiation of earthquakes, using hourly precipitation data. The models can be effective tools for detecting vulnerable slopes and establishing effective evacuation systems for deep-seated landslide events.

ACKNOWLEDGMENT: This work was partly supported by grants from MLIT, and the Fund of Monbukagakusho for Scientific Research (22248018, 23221009).

REFERENCES

Akaike, H. (1973): Information theory and an extension of the maximum likelihood principle, Petrov B.N. and Caski F. (eds.) Proc. of 2nd International Symposium on Information Theory, Akadimiai Kiado, Budapest, pp.267-281.

Chigira, M., Nakasuji, A., Fujiwara, S. and Sakagami, M. (2012): Soilslide-avalanches of pyroclastic fall deposits induced by the 2011 off the Pacific coast of Tohoku earthquake, J. Jpn. Soc. Eng. Geol., Vol. 52, No. 6, pp. 222-230 (in Japanese with English abstract).

Descroix, L., Nouvelot, J.-F. and Vauclin, M. (2002): Evaluation of an antecedent precipitation index to model runoff yield in the western Sierra Madre (North-west Mexico), J. Hydrol., Vol. 263, pp. 114-130.

Fedora, M.A., and Beschta, R.L. (1989): Storm runoff simulation using an antecedent precipitation index (API) model, J. Hydrol., Vol. 112, pp. 121-133.

Jitousono, T., Shimokawa, E., Sako, M. and Teramoto, Y. (2004): Hydrogeomorphological characteristics of a deep-seated landslide in the Harihara river basin, Izumi city, Kagoshima prefecture, Japan, J. Jpn. Soc. Erosion Control. Eng., Vol. 56, No. 5., pp. 15-26 (in Japanese with English abstract).

Kosugi, K., Fujimoto, M., Yamakawa, Y., Masaoka, N., Itokazu, T., Mizuyama, T. and Kinoshita, A. (2013): Functional models correlating antecedent precipitation indices to bedrock groundwater levels, Japan, J. Jpn. Soc. Erosion Control. Eng., Vol. 66, No. 4., pp. 21-32 (in Japanese with English abstract).

Kosugi, K., Kinoshita, A., Fujimoto, M., Mizuyama, T. and Sando Y. (2012): Problems on shallow landslide predictions based on topographically-driven rainwater convergences, J. Jpn. Soc. Erosion Control. Eng., Vol. 65, No. 1., pp. 27-38 (in Japanese with English abstract).

Kosugi, K. Sando, Y., Fujimoto, M., Yamakawa, Y., Masaoka, N., Mizuyama, T., Hiramatsu, S., Fukuyama, T. and Jitousono, T. (2014): Analyses of bedrock groundwater levels as a factor of deep landslides by using functional models, Japan, J. Jpn. Soc. Erosion Control. Eng., Vol. 66, No. 6., pp. 3-14 (in Japanese with English abstract).

Niigata Prefecture Civil Engineering Division (2005): Sediment disasters caused by the mid Niigata prefecture earthquake in 2004, Niigata Prefecture Civil Engineering Division and SABO Technical Center, pp. 7-13 (in Japanese, the title is a tentative translation by the authors of this paper).

Sittner, W.T., Schauss, C.E. and Monro, J.C. (1969): Continuous hydrograph synthesis with an API-type hydrologic model, Water Resour. Res., Vol. 5, pp. 1007-1022.

Suzuki, M. and Kobashi, S. (1981): The critical rainfall for the disasters caused by slope failures, J. Jpn. Soc. Erosion Control. Eng., Vol. 34, No. 2, pp. 16-26 (in Japanese with English abstract).

Tsutsumi, D. and Fujita, M. (2012): Effects of soil moisture condition on slope-stability reductions caused by earthquakes, Proc. Annual JSECE Meeting, JSECE Pub. No. 66, pp. 356-357 (in Japanese, the title is a tentative translation by the authors of this paper).